Supporting Information
for
Half-projected σ-SCF For Electronic Excited States

Hong-Zhou Ye[1] and Troy Van Voorhis[*1]

[1] *Department of Chemistry, Massachusetts Institute of Technology, Cambridge, MA, 02139*

Note: figures, tables, and etc. in the main text are referred as Figure Mxxx, Table Mxxx, and etc.

S1   Expressions of HP σ-SCF Fock matrices

In eqn (M23), $(\boldsymbol{\mathcal{F}}_\eta^s)_1$ arises from differentiating σ_1^2 and E_1 in σ_η^2,

$$(\boldsymbol{\mathcal{F}}_\eta^s)_1 = \boldsymbol{\mathcal{F}}^s + \frac{2\eta D(E_1 - E_2)}{1 + \eta D}\boldsymbol{F}^s, \tag{S1}$$

and $(\boldsymbol{\mathcal{F}}_\eta^s)_2$ and its hermitian conjugate arise from differentiating σ_2^2, E_2, and D in σ_η^2,

$$(\boldsymbol{\mathcal{F}}_\eta^s)_2 = \boldsymbol{Q}^{s\bar{s}}\left[\boldsymbol{\mathcal{F}}^{\bar{s}s} - \frac{2(E_1 - E_2)}{1 + \eta D}\boldsymbol{F}^{\bar{s}s}\right]\boldsymbol{P}^{s\bar{s}} + \\ \frac{1}{1 + \eta D}\left[\sigma_2^2 - \sigma_1^2 + \frac{1 - \eta D}{1 + \eta D}(E_1 - E_2)^2\right]\boldsymbol{P}^{s\bar{s}}. \tag{S2}$$

In the equations above,

$$\begin{aligned}\mathcal{F}_{\mu\nu}^s = &[\boldsymbol{F}^s(\boldsymbol{Q}^s - \boldsymbol{P}^s)\boldsymbol{F}^s]_{\mu\nu} + \\ &(\mu\nu|\lambda\sigma)(\mathcal{P}_{\sigma\lambda}^s + \mathcal{P}_{\sigma\lambda}^{\bar{s}}) - (\mu\sigma|\lambda\nu)\mathcal{P}_{\sigma\lambda}^s + \\ &(Q_{\lambda\lambda'}^s P_{\sigma\sigma'}^s Q_{\gamma\gamma'}^s - P_{\lambda\lambda'}^s Q_{\sigma\sigma'}^s P_{\gamma\gamma'}^s)\times \\ &(\mu\lambda|\sigma\gamma)[(\nu\lambda'|\sigma'\gamma') - (\nu\gamma'|\sigma'\lambda')] + \\ &(Q_{\lambda\lambda'}^s P_{\sigma\sigma'}^{\bar{s}} Q_{\gamma\gamma'}^{\bar{s}} - P_{\lambda\lambda'}^s Q_{\sigma\sigma'}^{\bar{s}} P_{\gamma\gamma'}^{\bar{s}})\times \\ &(\mu\lambda|\sigma\gamma)(\nu\lambda'|\sigma'\gamma')\end{aligned} \tag{S3}$$

are the σ-SCF Fock matrices, where $\boldsymbol{\mathcal{P}}^s = \boldsymbol{P}^s\boldsymbol{F}^s\boldsymbol{Q}^s + \boldsymbol{Q}^s\boldsymbol{F}^s\boldsymbol{P}^s$, and

$$\begin{aligned}\mathcal{F}_{\mu\nu}^{s\bar{s}} = &[\boldsymbol{F}^{\bar{s}s}(\boldsymbol{Q}^{s\bar{s}} - \boldsymbol{P}^{s\bar{s}})\boldsymbol{F}^{\bar{s}s}]_{\mu\nu} + \\ &(\mu\nu|\lambda\sigma)(\mathcal{P}_{\sigma\lambda}^{s\bar{s}} + \mathcal{P}_{\sigma\lambda}^{\bar{s}s}) - (\mu\sigma|\lambda\nu)\mathcal{P}_{\sigma\lambda}^{s\bar{s}} + \\ &(Q_{\lambda\lambda'}^{\bar{s}s} P_{\sigma\sigma'}^{s\bar{s}} Q_{\gamma\gamma'}^{\bar{s}s} - P_{\lambda\lambda'}^{\bar{s}s} Q_{\sigma\sigma'}^{s\bar{s}} P_{\gamma\gamma'}^{\bar{s}s})\times \\ &(\mu\lambda|\sigma\gamma)[(\nu\lambda'|\sigma'\gamma') - (\nu\gamma'|\sigma'\lambda')] + \\ &(Q_{\lambda\lambda'}^{\bar{s}s} P_{\sigma\sigma'}^{s\bar{s}} Q_{\gamma\gamma'}^{\bar{s}s} - P_{\lambda\lambda'}^{\bar{s}s} Q_{\sigma\sigma'}^{s\bar{s}} P_{\gamma\gamma'}^{s\bar{s}})\times \\ &(\mu\lambda|\sigma\gamma)(\nu\lambda'|\sigma'\gamma')\end{aligned} \tag{S4}$$

are the cross σ-SCF Fock matrices with a similar definition for $\mathcal{P}^{s\bar{s}}$ as above.

---

[*]tvan@mit.edu

S2 Expressions of HP σ-SCF DET Fock matrices

The DET Fock matrices of HP σ-SCF have the following form,

$$\boldsymbol{f}_\eta^s(\omega) = \boldsymbol{\mathcal{F}}_\eta^s + 2(E_\eta - \omega)\boldsymbol{F}_\eta^s, \tag{S5}$$

where $\boldsymbol{\mathcal{F}}_\eta^s$ is the HP σ-SCF Fock matrix [eqn (M23)];

$$\boldsymbol{F}_\eta^s = \boldsymbol{F}^s + \eta D[(\boldsymbol{F}_\eta^s)_2 + (\boldsymbol{F}_\eta^s)_2^\dagger] \tag{S6}$$

is the HPHF Fock matrix, with

$$(\boldsymbol{F}_\eta^s)_2 = \boldsymbol{F}^{s\bar{s}} + \frac{E_2 - E_1}{1 + \eta D}\boldsymbol{P}^{s\bar{s}}. \tag{S7}$$

Note that eqn (S6) is consistent with the result obtained in Ref. [1].

S3 Some properties of HP methods

Here, we present formal discussion of some properties of HP methods, which complements our discussion in Sec. M2.5.

As a HP method, HP σ-SCF improves upon the original σ-SCF in two ways: reducing the spin-contamination and recovering some static correlation energy. To see the effect of half-projection on spin-contamination, we first introduce the so-called corresponding orbitals,[2]

$$\langle \tilde{\phi}_i^\alpha | \tilde{\phi}_j^\beta \rangle = \lambda_i \delta_{ij}, \qquad \lambda_i \in [0, 1] \tag{S8}$$

which are related to the occupied MOs by a unitary rotation determined from the singular value decomposition of $\boldsymbol{S}^{\alpha\beta}$ [eqn (M13)], with $\{\lambda_i\}$ being the singular values. In terms of these orbitals, D has a simple product form,

$$D = \prod_{i=1}^N \lambda_i^2. \tag{S9}$$

With these orbitals, the total spin expectation can be readily computed for both the unprojected and the HP wave functions:[1]

$$\langle \Phi | \hat{S}^2 | \Phi \rangle = N - \sum_{i=1}^N \lambda_i^2, \tag{S10}$$

and

$$\frac{\langle \Psi_\eta | \hat{S}^2 | \Psi_\eta \rangle}{\langle \Psi_\eta | \Psi_\eta \rangle} = N - (1 + \eta D)^{-1} \sum_{i=1}^N (\lambda_i^2 + \eta D \lambda_i^{-2}). \tag{S11}$$

Since $\lambda_i \leq 1$ for all i's, $\langle \hat{S}^2 \rangle$ of Ψ_η is always closer to the value of a pure spin state (i.e., 0 for singlet and 2 for triplet) compared to that of Φ, demonstrating that half-projection reduces spin-contamination. The correlation energy, on the other hand, can be read directly from eqn (M6) if the orbitals are assumed to be frozen,

$$E_\eta - E_1 = \frac{\eta D(E_2 - E_1)}{1 + \eta D}, \tag{S12}$$

which takes opposite signs for singlet ($\eta = +1$) and triplet ($\eta = -1$), hence capable of opening the energy gap between them. Due to the two-determinant nature of the HP wave function, this correction mainly affects the static correlation energy.

The magnitude of both the spin and the energy corrections induced by half-projection is controlled by the magnitude of $\{\lambda_i\}$ [and hence the magnitude of D due to eqn (S9)]. At one extreme where all λ_i's are equal to 1, the HP wave function reduces to a RHF/R σ-SCF state, which has no spin-contamination but no energy correction either ($E_2 = E_1$ in this case). At the other extreme where $\lambda_i \sim 0$ for many i's, the HP wave function tends to the unprojected UHF/U σ-SCF state, with both the spin and the energy corrections tending to zero according to eqns (S10) – (S12). Note that when there it only one $\lambda_i \sim 0$, the singularity can be removed algebraically.[1]

We further note the limitation of half-projection by analysis of the NO occupation numbers. Suppose the number of electrons is less than the size of basis functions (i.e., $2N < K$, which is the case for

moderate- and large-sized bases). Then for both the the unprojected and the HP wave functions, there are exactly $2N$ NOs that are occupied; these NOs take the following paired form in terms of the corresponding orbitals in eqn (S8),[1]

$$\psi_i^\pm = \frac{1}{\sqrt{2(1 \pm \lambda_i)}}(\tilde{\phi}_i^\alpha \pm \tilde{\phi}_i^\beta). \tag{S13}$$

The effect of half-projection lies in altering the NO occupation numbers, with $n_i^\pm = 1 \pm \lambda_i$ before and

$$(n_i^\pm)_\eta = (1 + \eta D)^{-1}[1 \pm \lambda_i + \eta D(1 \pm \lambda_i^{-1})] \tag{S14}$$

after the projection, without increasing the number of partially occupied NOs. Thus, the HP wave function could fail in providing a qualitative description of the electronic structure if a large number of NOs (e.g., $> 2N$) are populated in the exact solution. Nevertheless, as demonstrated in Sec. M4.1, these strongly correlated states can be described by invoking a NOCI calculation based on the HP σ-SCF solutions.

S4 σ-SCF solutions of 3-21G H_2

Shown in Figure S1 are the unprojected σ-SCF excited-state solutions for $M_s = 0$ states of 3-21G H_2. R and U σ-SCF stand for spin-restricted and spin-unrestricted, respectively. One can see that

(i) the spin-contamination makes they U σ-SCF solutions a good approximation to neither the singlet nor triplet FCI states;

(ii) several solutions disappear beyond some bond length;

(iii) the potential energy surface (PES) of one solution is kinked (d(H-H) ≈ 0.7 Å, $E_{\text{tot}} \approx 1.0$ Ha).

All three problems have been fixed after the half-projection (see Figure M1).

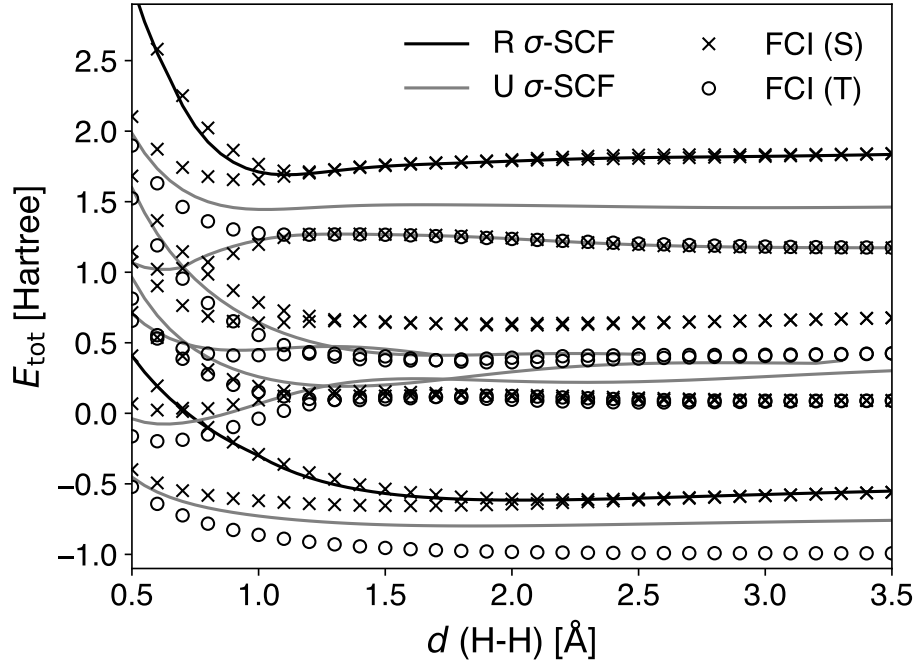Figure S1: $M_s = 0$ excited-state solutions found by σ-SCF for 3-21G H_2 compared to FCI.

S5   NOCI based on HP σ-SCF solutions of 3-21G H_2

In the main text, we mention that several FCI states of 3-21g H_2 are truly multi-reference at stretched geometries, with all natural orbitals (NOs) displaying fractional occupation. In such cases, HP σ-SCF, being a two-determinant theory, fails to capture the qualitative behavior of the FCI solutions, as can be seen from the mismatch of the blue curves and black crosses in Figure S2.

Fortunately, since these HP σ-SCF solutions exist at all bond lengths, we can recover the missing static correlation by invoking a non-orthogonal configuration interaction (NOCI) calculation using them as bases. As shown in Figure S2, the four singlet HP σ-SCF solutions (all preserving the mirror symmetry) are divided into two groups[1], each containing two HP solutions (blue solid and blue dashed curves, respectively). Two-state NOCI calculations are performed for each group and the results are shown in green in Figure S2 (solid and dashed, respectively). From the figure, one can see that NOCI manages to capture the behavior of the FCI solutions in a quantitative manner.
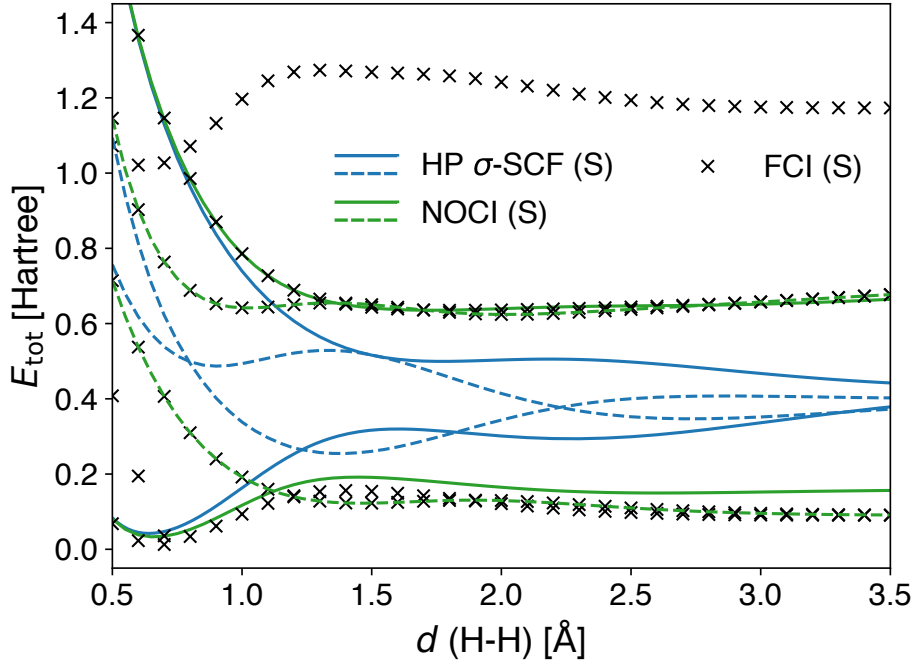

Figure S2: PESs obtained by NOCI (green) using selected HP σ-SCF singlet states (blue) as quasi-diabatic bases. FCI solutions (black) are also included for comparison.

---

[1]A more common way would be to include all four states in one NOCI calculation. However, for this specific case, the matrix elements between states that belong to different groups vanish because of the orbitals symmetry. In other words, our results here will be exactly equivalent to a four-state NOCI calculation.

S6 σ-SCF solutions of 3-21G LiH

Shown in Figure S3 are the unprojected σ-SCF excited-state solutions for the first several $M_s = 0$ states of 3-21G LiH. One can see that

  (i) R σ-SCF dissociates LiH into a high-energy, ionic state which has the incorrect asymptotic behavior;

 (ii) there is a spurious σ-SCF solution in between the first two FCI triplet states that does not correspond to any physical states;

(iii) several solutions disappear in the intermediate energy range.

As can be seen from the main text (FIG. M3), the first two problems are solved by HP σ-SCF, while the last one is mitigated greatly by HP σ-SCF.
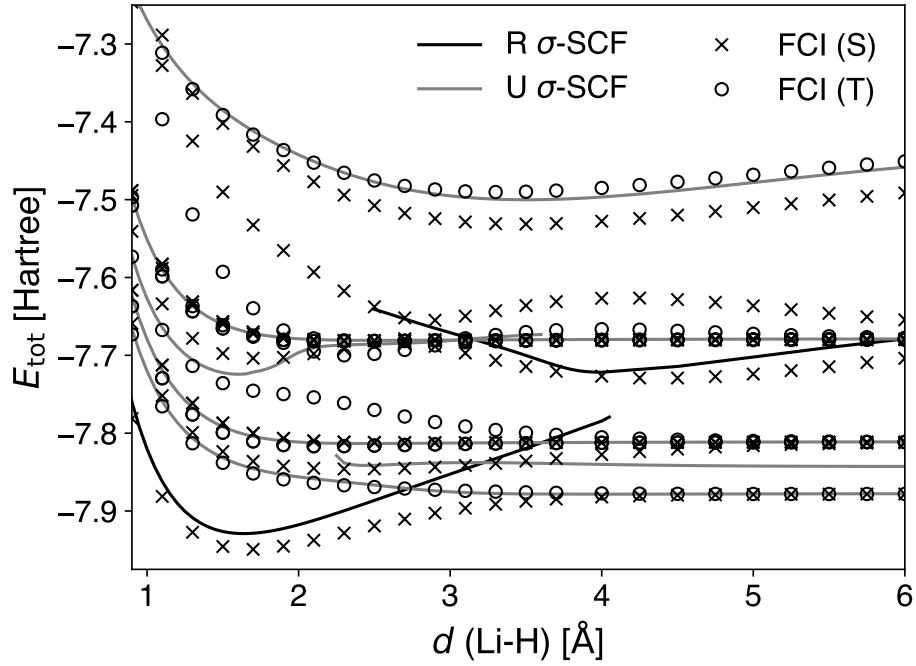

Figure S3: First several $M_s = 0$ excited-state solutions found by σ-SCF for 3-21G LiH compared to FCI.

S7 σ-SCF solutions of STO-3G C_2H_4

Shown in Figure S4 are the unprojected σ-SCF excited-state solutions for the first several $M_s = 0$ states of STO-3G C_2H_4. One can see that

(i) for ground states, the R σ-SCF solution is in parallel to the FCI singlet solution for small θ but curves upward for large θ, revealing its missing static correlation;

(ii) the U σ-SCF ground-state solution, on the other hand, has too flat of curvature due to the strong spin-contamination from the first triplet state;

(iii) for excited states, the dense feature of the FCI spectrum is produced, but the σ-SCF solutions disappear at several places.

As can be seen from the main text (FIG. M4), the first two problems are solved by HP σ-SCF, while the last one is mitigated greatly by HP σ-SCF.
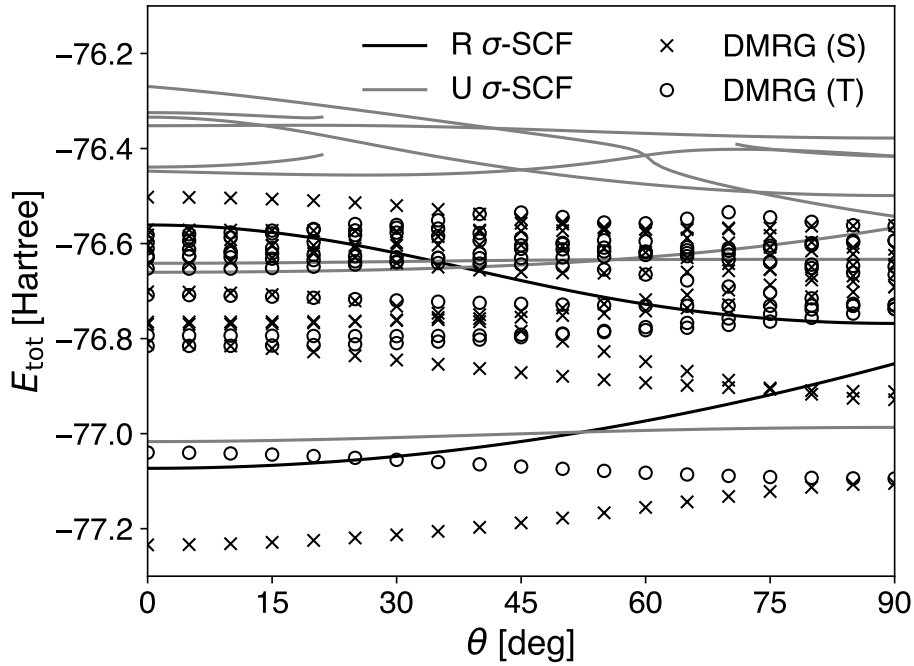

Figure S4: First several $M_s = 0$ excited-state solutions found by σ-SCF for STO-3G C_2H_4 compared to FCI.

References

[1] P. Anthony Cox and Melvyn H. Wood. The half-projected hartree-fock method. i. eigenvalue formulation and simple applications. *Theoret. Chim. Acta*, 41(4):269–278, Dec 1976.

[2] A. T. Amos and G. G. Hall. Single determinant wave functions. *Proc. R. Soc. Lond. A*, 263(1315):483–493, 1961.